Scale-reduction rule for diaphragm dimensions to miniaturize a silicon-based integrated optic pressure sensor without reducing sensitivity

Atsushi Yamada[a], Tooru Tokita[a], Masashi Ohkawa*[b], Seishi Sekine[b], and Takashi Sato[b]

[a]Niigata University, Graduate School of Science and Technology, Ohkawa Lab.
8050 Ikarashi 2-no-cho, Niigata 950-2181, Japan
[b]Niigata University, Faculty of Engineering
8050 Ikarashi 2-no-cho, Niigata 950-2181, Japan

ABSTRACT

In this paper, an original scale-reduction rule without sensitivity loss in integrated optic pressure sensors based on the elasto-optic effect is described. The sensor has a rectangular diaphragm as a pressure-sensitive mechanical structure and a sensing waveguide on the diaphragm. In this type of sensor, sensitivity is theoretically known to be strongly dependent on the dimensions of the diaphragm. According to the theoretical results, the sensitivity can be kept constant even if the diaphragm dimensions are reduced as long as both the side length ratio and the characteristic length remain constant. Here, the characteristic length is introduced as the cube of the shorter side length of the diaphragm divided by the square of the thickness. Such a scale-reduction rule would be very significant in the miniaturizing of a sensor without reducing sensitivity, but it has not been experimentally confirmed. In this study, the scale-reduction rule was experimentally examined using three fabricated sensors, which had the same side length ratio and the same characteristic length. The exact dimensions of the sensors were 2.0 mm×10 mm×35 μm, 2.5 mm×12.5 mm×49 μm and 3.0 mm×15 mm×64 μm. The measured sensitivities of the three sensors were quite similar to each other as theoretically predicted.

Keywords: integrated optics, pressure sensor, elasto-optic effect, silicon, diaphragm

1. INTRODUCTION

In the past decade, micro-opto-mechanical devices have received considerable attention in the development of silicon micro-machining technology.[1] An integrated optic pressure sensor with a micro-machined diaphragm is one of the promising micro-opto-mechanical devices. Several groups have reported on the integrated optic pressure sensors with diaphragms since the late 1980's.[2-5] Our group has been developing a silicon-based integrated optic pressure sensor using intermodal interference between the fundamental TM-like and TE-like modes.[6, 7] One of the targets of our study is the realization of a sensor that can be incorporated into a catheter to measure blood pressure. For this target, it is very significant to miniaturize the sensor while keeping sensitivity constant. The sensitivity of the sensor is theoretically known to be proportional to the cube of the length of either side of the rectangular diaphragm. Also, the sensitivity is inversely proportional to the square of the thickness of the diaphragm. From these dependencies, an original scale-reduction rule without sensitivity loss can be derived, in other words sensitivity can be maintained when the diaphragm dimensions are reduced by keeping the side length ratio and the characteristic length constant. Here, the characteristic length is defined as the cube of the shorter side length of the diaphragm divided by the square of the thickness. To confirm the scale-reduction rule experimentally, three sensors were fabricated with the same side length ratio and the same characteristic length. The exact dimensions of the sensors were 2.0 mm×10 mm×35 μm for sensor #1, 2.5 mm×12.5 mm×49 μm for sensor #2 and 3.0 mm×15 mm×64 μm for sensor #3, so the side length ratio was 1:5 and the characteristic length was about 6.5 m. The sensitivities of sensors #1, #2 and #3 were 71, 72, 69 mrad/kPa, respectively, for the waveguide nearest to the center of the diaphragm at a wavelength of 633 nm. For the corresponding waveguide positions of the three sensors, the measured sensitivities were quite similar to each other as predicted by the scale-reduction rule. The scale-reduction rule can be applied to any integrated optic pressure sensors with a diaphragm based on the elasto-optic effect.

Integrated Optics: Devices, Materials, and Technologies VII, Yakov S. Sidorin, Ari Tervonen, Editors, Proceedings of SPIE Vol. 4987 (2003) © 2003 SPIE · 0277-786X/03/$15.00

2. PRINCIPLE OF SENSOR OPERATION

Figure 1 shows an integrated optic pressure sensor utilizing intermodal interference between the fundamental TM-like and TE-like modes. The sensor consists of a rectangular diaphragm and a straight single-mode waveguide over the diaphragm. The diaphragm is distorted when a pressure difference is applied. The distortion causes strain, which induces a change in the refractive index of the diaphragm by the elasto-optic effect. The index change yields phase retardation in the lightwave propagating in the waveguide on the diaphragm. Since the phase retardation is generally dependent on the guided modes, the phase difference between the two modes is also a function of the applied pressure. To detect the phase difference, the sensor is placed between a pair of crossed polarizers as shown in Fig. 2. The polarization axis of the input polarizer is oriented at 45° with respect to the polarization of each guided modes, so that the laser beam is coupled to the TM-like and TE-like modes at equal intensities The lightwave has linear, elliptic or circular polarization at the end of the waveguide, corresponding to the induced phase difference between the two guided modes. The intensity of the light beam passing through the output polarizer sinusoidally changes with the applied pressure. Therefore, the applied pressure can be determined from the output intensity.

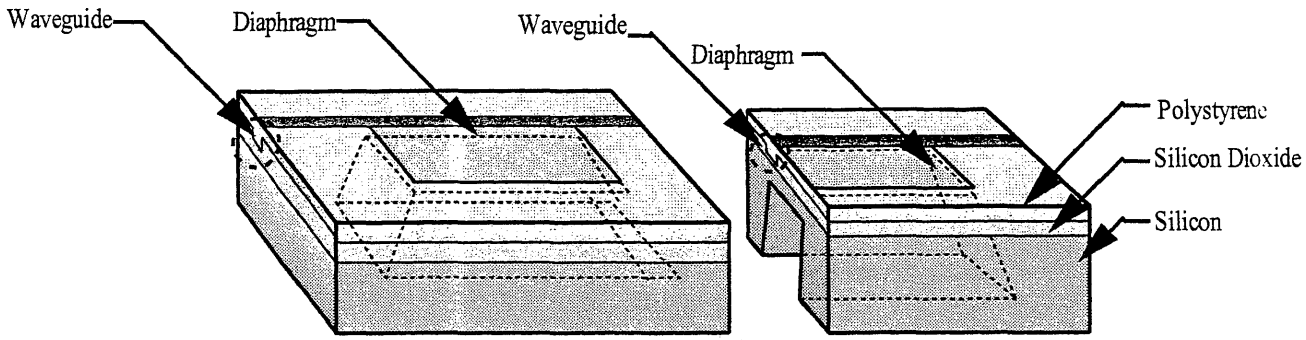

Fig. 1 Schematic drawing of the integrated optic pressure sensor using intermodal interference.

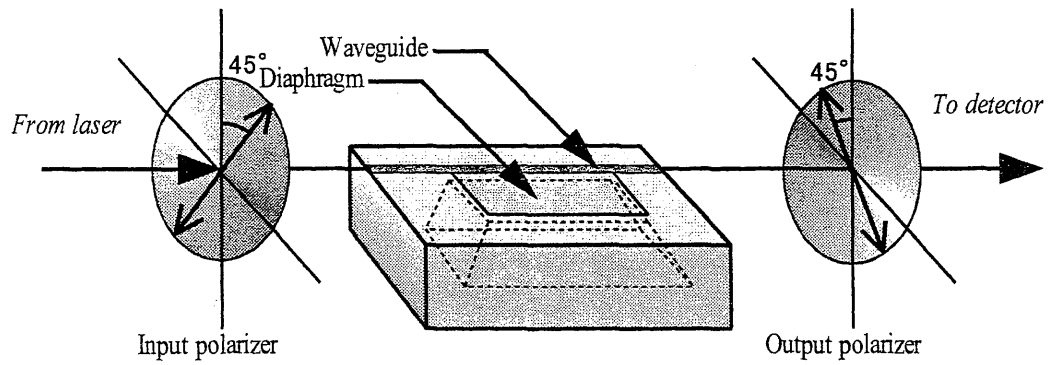

Fig. 2 A sensor placed between a pair of crossed polarizers to convert polarization-modulated light into intensity-modulated light.

3. THEORETICAL RESULTS

3.1 Dependence of sensitivity on diaphragm dimensions

3.1.1 Sensitivity versus area of diaphragm

The phase sensitivity, that is, the phase difference per unit pressure, is strongly dependent on the area of the diaphragm. The phase sensitivity was calculated, following the mathematical description in Ref. 7, as a function of the side length of the rectangular diaphragm while keeping the side length ratio and diaphragm thickness constant. In the calculation, a rectangular diaphragm with an area of $a \times b$ and a thickness of t was assumed. It was also assumed that the waveguide was placed parallel to side b and the pressure was uniformly applied over the diaphragm with all edges rigidly clamped. The wavelength of the guided light was set at 633 nm. Incidentally, theoretical calculations should be carried out using the mechanical and optical parameters of the materials that comprise the sensor. However, the parameters for polystyrene, which is the material used for the guided layer of the waveguide shown in Fig. 1, have yet to be determined. In this study, the parameters of fused silica were used instead of those of polystyrene. The numerical result obtained by using the parameters of fused silica would qualitatively hold true for a sensor using a polystyrene waveguide.

Figure 3 indicates the calculated phase sensitivity versus the side length a. Sensitivity is normalized to be at unity at a side length of 1mm. From Fig. 3, the slope is 3 in log-log graph, so that the sensitivity is proportional to the cube of the side length of the diaphragm. The relationship between the normalized phase sensitivity and the side length is valid for the arbitrary side length ratio and thickness of the diaphragm. This relationship can be also applied to any waveguide position although the waveguide was assumed to be located along the edge of the diaphragm in the calculation.

3.1.2 Sensitivity versus thickness of diaphragm

The phase sensitivity was calculated as a function of the diaphragm thickness, with the other dimensions remaining constant. Figure 4 shows the calculated phase sensitivity versus the thickness. The phase sensitivity is normalized to be at unity at a thickness of 10 μm. In the figure, the slope is –2 in log-log graph when the diaphragm thickness is considerably greater than the waveguide thickness, which is assumed to be 1 μm. Therefore, the sensitivity is inversely proportional to the square of the diaphragm thickness. When the diaphragm thickness is comparable to or less than the spread of the guided light in the direction of the thickness, the sensitivity decreases as the diaphragm thins because the overlap integral between the electric field of the guided light and the refractive index change becomes smaller.[7] Such thin diaphragms should not be considered when designing the sensors.

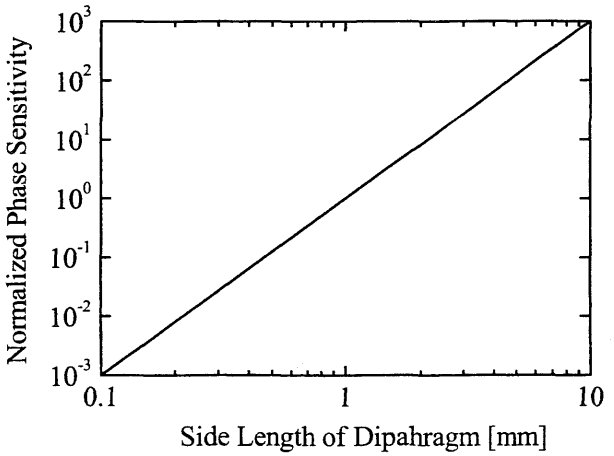

Fig. 3 Calculated phase sensitivity as a function of the side length of the diaphragm. The phase sensitivity is normalized to be at unity at a side length of 1 mm.

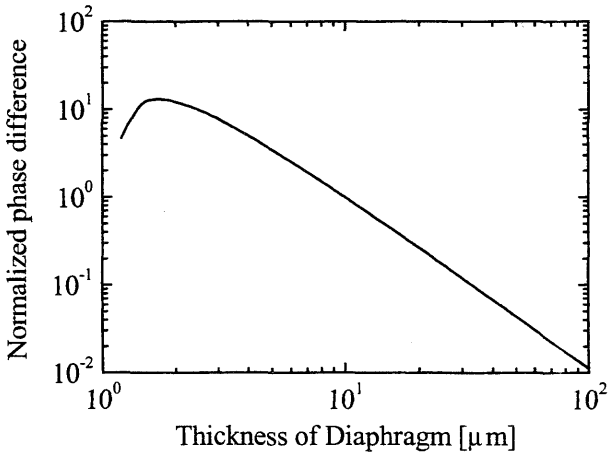

Fig. 4 Calculated normalized phase sensitivity as a function of the thickness of the diaphragm. The phase sensitivity is normalized to be at unity at 10 μm in thickness.

3.2 Scale-reduction rule

To design a miniaturized sensor, a scale-reduction rule of diaphragm dimensions without sensitivity loss is very helpful, especially when the present sensor is sufficiently sensitive but sizable. From Section **3.1.1**, it is found that sensitivity is proportional to the cube of the side length if the side length ratio and the thickness remain constant. Also, from Section **3.1.2**, sensitivity is inversely proportional to the square of the thickness when the side length ratio and the area are both kept constant. Here, the characteristic length a^3/t^2 is introduced, defined by the cube of the shorter side length of the diaphragm divided by the square of the thickness. From the two theoretical results, sensitivity can remain constant, even if the diaphragm dimensions are reduced, as long as both the side length ratio and the characteristic length remain constant.

4. EXPERIMENT

4.1 Fabrication and measurement

We fabricated three sensors with a diaphragm of 2.0 mm×10 mm×35 μm (sensor #1), 2.5 mm×12.5 mm×49 μm (sensor #2), or 3.0 mm×15 mm×64 μm (sensor #3) to confirm the scale-reduction rule mentioned above. The waveguides were spaced 0.1mm apart from each other to concurrently determine how phase sensitivity is related to waveguide position. In fabrication, a silicon substrate was thermally oxidized at 1100 °C to form a silicon dioxide layer. The silicon dioxide layer was selectively removed with an etchant of buffered HF acid using a patterned photoresist as an etching mask. Then, the exposed silicon was anisotropically etched by KOH to produce the diaphragm. After diaphragm formation, the silicon dioxide layer was grown to a thickness of 1.0 μm by thermal oxidation to serve as a buffer to sufficiently negate radiation loss of the guided waves in the silicon substrate. Shallow 10μm-wide and 0.1mm-deep grooves were engraved on the silicon dioxide layer, parallel to the diaphragm edge using buffered HF acid. The polystyrene layer was spin-coated as the guided layer, and its thickness at the grooves was 1.1 μm.

Figure 5 illustrates the experimental setup to measure output intensity versus applied pressure. In the measurement, a linearly-polarized He-Ne laser at 633 nm was used, and its polarization was set at 45° to the sensor surface without using the input polarizer shown in Fig. 2. A pressure difference, ranging from –40 kPa to 40 kPa, was exerted on the diaphragm by pulling and pushing on the plunger of the syringe connected to the sensor by a silicone tube. A positive value represents that the pressure in the etched hole is higher than that in the atmosphere.

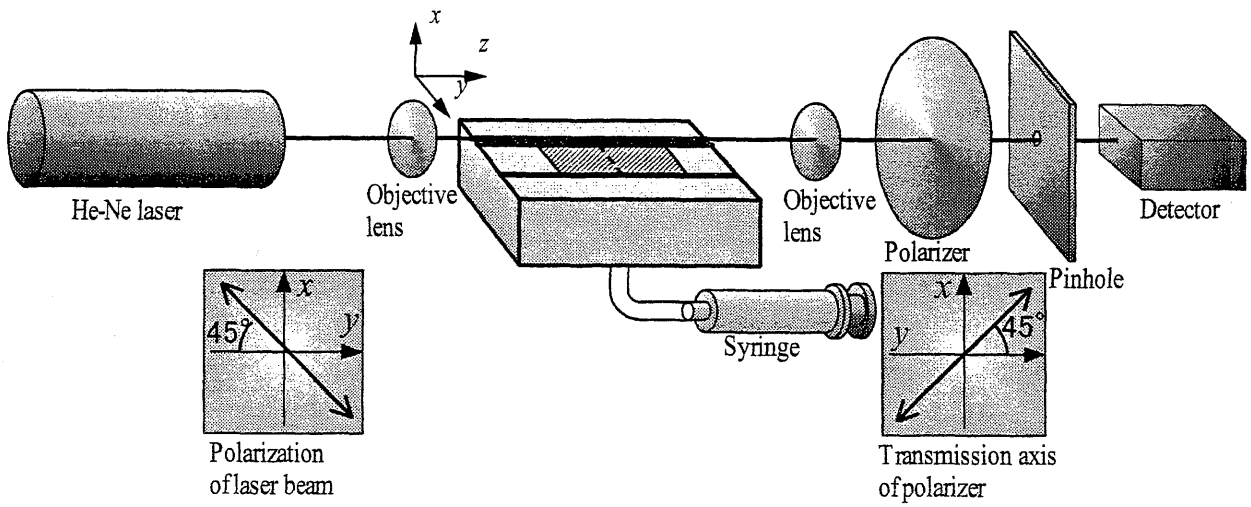

Fig. 5 Experimental setup to measure the output intensity with respect to the applied pressure.

4.2 Experimental results

4.2.1 Experimental results of sensor #1 with 2.0 mm×10 mm×35 μm diaphragm

Figure 6 shows the experimental results of sensor #1 with a 2.0 mm×10 mm×35 μm diaphragm. Figures 6(a) and (b) are for the waveguides nearest to the diaphragm edge and nearest to the center of the diaphragm, respectively. The solid line in each figure shows the computer projection of the experimental data. The halfwave pressure is evaluated as a half period of the output intensity, corresponding to a phase difference of π rad. From the halfwave pressure, the phase sensitivity, defined as the resultant phase difference per unit pressure, is calculated. From Figs. 6(a) and (b), the halfwave pressures are 36kPa and 44kPa, and the corresponding phase sensitivities are calculated to be 89mrad/kPa and 71mrad/kPa, respectively. Moreover, the phase sensitivities of the other waveguide positions were also measured. Figure 7 indicates the measured phase sensitivities as a function of the waveguide position. Several data points are missing due to imperfect waveguides. In Fig. 7, the theoretical curve reflects the calculated results when the side length ratio *a/b* of the rectangular diaphragm is 0.2. The sign of the measured phase sensitivity was determined based on the theoretical sensitivity although it cannot be distinguished in these experimental results.

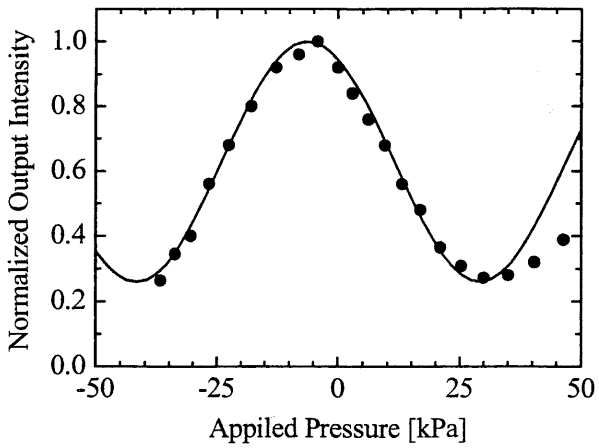

Fig. 6(a) Measured output intensity versus applied pressure for the waveguide nearest to the diaphragm edge.

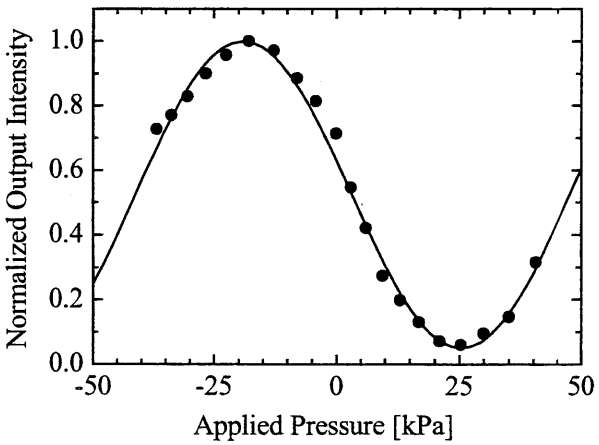

Fig. 6(b) Measured output intensity versus applied pressure for the waveguide located nearest to the center of the diaphragm.

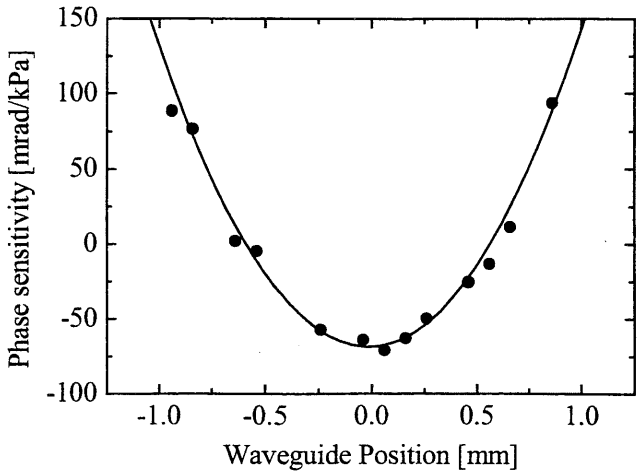

Fig. 7 Measured sensitivity as a function of waveguide position. Waveguide positions of ± 1.0 mm approximately correspond to the edge of the diaphragm, while a waveguide position of 0 mm corresponds to the center.

4.2.2 Experimental results of sensor #2 with 2.5 mm×12.5 mm×49 μm diaphragm

Figures 8(a) and (b) show the experimental results of sensor #2 with a 2.5 mm×12.5 mm×49 μm diaphragm for the waveguides located nearest to the edge and nearest to the center of the diaphragm, respectively. From Figs. 8(a) and (b), the halfwave pressures are 29 kPa and 44 kPa, corresponding to the sensitivities of 110 mrad/kPa and 72 mrad/kPa, respectively. Figure 9 shows the measured sensitivity versus the waveguide position. Several data points are missing due to imperfect waveguides, similar to the results of sensor #1. The solid curve in the figure indicates the computer projection when $a/b = 0.2$.

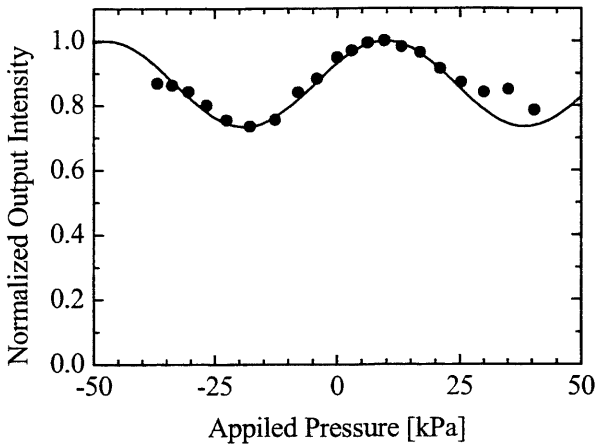

Fig. 8(a) Measured output intensity versus applied pressure for the waveguide nearest to the diaphragm edge.

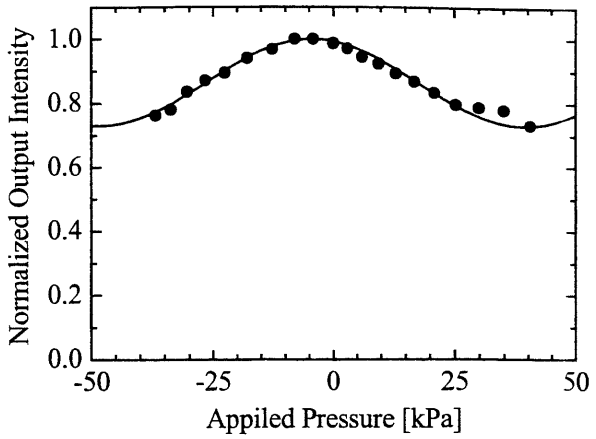

Fig. 8(b) Measured output intensity versus applied pressure for the waveguide located nearest to the center of the diaphragm.

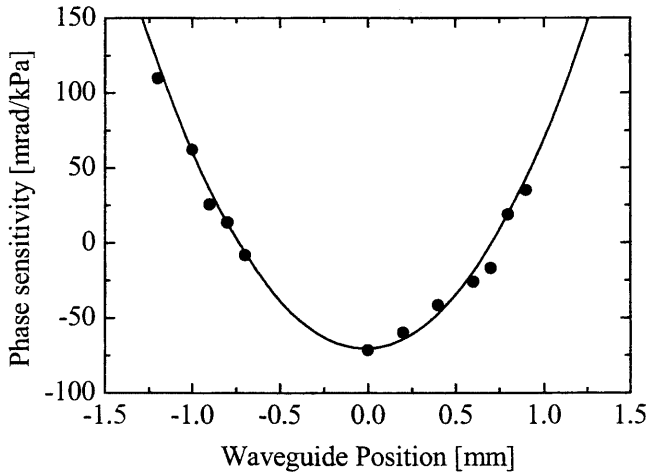

Fig. 9 Measured sensitivity as a function of waveguide position. Waveguide positions of ± 1.25 mm approximately correspond to the edge of the diaphragm, while a waveguide position of 0 mm corresponds to the center.

4.2.3 Experimental results of sensor #3 with 3.0 mm×15 mm×64 μm diaphragm

Figure 10 shows the experimental results of sensor #3 with a 3.0 mm×15 mm×64 μm diaphragm. The waveguides of Fig. 10(a) and (b) were located nearest to the diaphragm edge and nearest to the center, respectively. The halfwave pressure was evaluated 31 kPa and 46 kPa from Figs. 10(a) and (b), corresponding to sensitivities of 100mrad/kPa and 69mrad/kPa, respectively. Figure 11 shows the measured phase sensitivity versus the waveguide position, and the theoretical curve reflecting the calculated results in the case of $a/b = 0.2$.

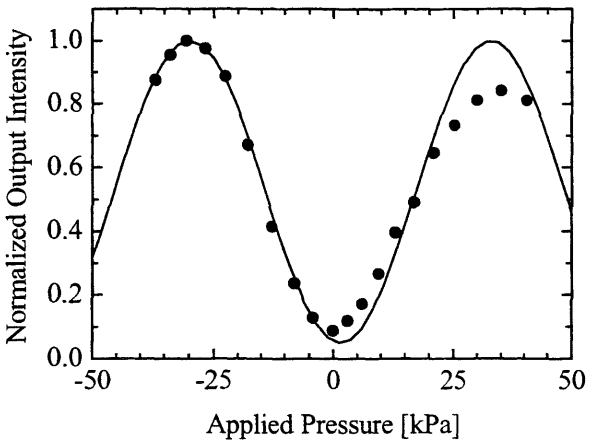

Fig. 10(a) Measured output intensity versus applied pressure for the waveguide nearest to the diaphragm edge.

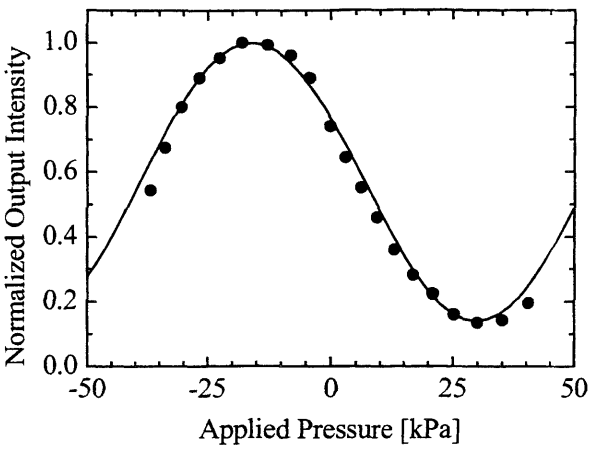

Fig. 10(b) Measured output intensity versus applied pressure for the waveguide located nearest to the center of the diaphragm.

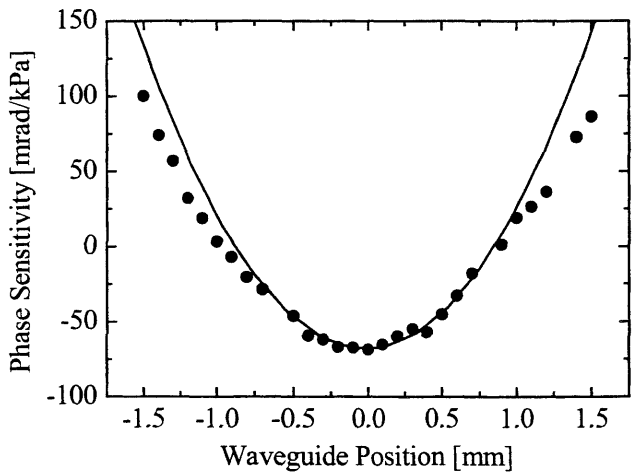

Fig. 11 Measured sensitivity as a function of waveguide position. Waveguide positions of ± 1.5 mm approximately correspond to the edge of the diaphragm, while a waveguide position of 0 mm corresponds to the center.

4.3 Discussions

In Figs. 7, 9 and 11, the relationships between the measured phase sensitivity and the waveguide position are almost identical with the theoretical ones although there is a slight difference near the diaphragm edge in Fig. 11. In each sensor, the largest sensitivity is obtained for the waveguide nearest to the diaphragm edge as theoretically predicted. The sensitivity, however, rapidly decreases as the waveguide deviates from the edge. In contrast, near the center of the diaphragm, small deviations in the waveguide minimally affect the sensitivity. By comparing the sensitivities among the fabricated sensors, the center of the diaphragm is better than the edge to avoid the effects of waveguide misalignment.

Table 1 shows the sensitivities of the fabricated sensors for the waveguides nearest to the edge and nearest to the center. Nearest to the center of the diaphragm, the measured sensitivities are quite similar to each other as predicted by the scale-reduction rule. Regarding the sensitivities nearest to the diaphragm edge, there is a difference of about 20 mrad/kPa. The difference was mainly caused by a deviation of the waveguide from the edge. Even for the measured sensitivities nearest to the edge, it is presumed that the sensitivities would be similar to each other, less error due to waveguide deviation. Therefore, the proposed scale-reduction rule is verified by the experimental results of the three fabricated sensors.

Table 1 Sensitivities of the three sensors with different diaphragm dimensions for the waveguides nearest to the edge and nearest to the center.

		Sensor #1	Sensor #2	Sensor #3
Diaphragm Dimensions	Width a [mm]	2.0	2.5	3.0
	Length b [mm]	10	12.5	15
	Thickness t [μm]	35	49	64
Side Length Ratio a / b		0.2		
Characteristic Length a^3 / t^2 [m]		6.5	6.4	6.6
Sensitivity for Waveguide nearest to Edge [mrad/kPa]		89	110	100
Sensitivity for Waveguide nearest to Center [mrad/kPa]		−71	−72	−69

5. CONCLUSIONS

We experimentally examined a scale-reduction rule without sensitivity loss in a silicon-based integrated optic pressure sensor. It was found theoretically and experimentally that sensitivity does not change even if the diaphragm dimensions are reduced as long as the side length ratio a/b and characteristic length a^3/b^2 remain constant. Incidentally, the obtained sensitivities for the three sensors are sufficient for blood pressure measurement, in which a phase sensitivity of about 80 mrad/kPa would be necessary. However, the sensors must be further miniaturized in order to be incorporated into a catheter. According to the scale-reduction rule, a sensor with a 0.5 mm×2.5 mm×4.4 μm diaphragm is expected to have the same sensitivity as the fabricated sensors, and could be put into a catheter. Moreover, for practical application, the objectives and the output polarizer in the experimental setup should be replaced with polarization-maintaining fibers attached to the two endfaces of the sensor. If a mirror is put on one endface instead of the fiber, the opposite endface can be used as the input and output port, creating a compact sensor with a pigtail polarization-maintaining fiber.

ACKNOWLEDGEMENT

This work is, in part, supported by a Grant-in-Aid for Scientific Research (No.12650339) from the Japan Society for the Promotion of Science.

REFERENCES

1. M. Tabib-Azar, and G. Beheim, "Modern trends in microstructures and integrated optics for communication, sensing, and actuation," Opt. Eng., **36**, pp.1307-1318, 1997.
2. M. Ohkawa, M. Izutsu, and T. Sueta, "Integrated optic pressure sensor on silicon substrate," Appl. Opt., **28**, pp.5153-5157, 1989.
3. G. N. De Brabander, J. T. Boyd, and G. Beheim, "Integrated optical ring resonator with micromechanical diaphragm for pressure sensing," IEEE Photon. Technol. Lett., **6**, pp.671-673, 1994.
4. G. N. De Brabander, Glenn Beheim, and J. T. Boyd, "Integrated optical micromachined pressure sensor with spectrally encoded output and temperature compensation," Appl. Opt., **37**, pp.3264-3267, 1998.
5. H. Porte, V. Gorel, S. Kiryenko, J. Goedgebuer, W. Daniau, and P. Blind, "Imbalanced Mach-Zehnder interferometer integrated in micromachined silicon substrate for pressure sensor," J. Lightwave Technol., **17**, pp.229-233, 1999.
6. M. Ohkawa, Y. Shirai, T. Goto, S. Sekine, and T. Sato, "Silicon-based integrated optic pressure sensor using intermodal Interference between TM-like and TE-like modes," Fiber and Integrated Optics, **21**, pp.105-113, 2002.
7. M. Ohkawa, K. Hasebe, S. Sekine, and T. Sato, "Relationship between sensitivity and waveguide position on the diaphragm in integrated optic pressure sensors based on the elasto-optic effect," Appl. Opt., **41**, pp.5016-5021, 2002.

*Correspondence: E-mail: ohkawa@eng.niigata-u.ac.jp; Telephone & Fax: +81-25-262-6734